of the Ni(II) ions in these protein active sites. By comparison, however, the urease magnetic data indicate additional perturbation of the Ni(II) ground state due to a weak exchange interaction between the two Ni(II) ions in the catalytically active subunit. Binding of thiolate inhibitors appears to result in a large antiferromagnetic interaction between the urease Ni(II) ions and suggests the possibility of bridging coordination of substrates. Additional studies of the magnetic and spectroscopic properties of this enzyme will further evaluate the Ni–Ni interaction to elucidate structural, electronic, and catalytic properties of the urease binuclear nickel active site.

Acknowledgment. We thank Richard Frankel for use of the SQUID magnetometer facility at the Francis Bitter National Magnet Laboratory, MIT, and Christopher Reed and Carol Koch for assistance with the USC SQUID magnetometer purchased with funding from the NSF. We thank Edmund Day for a preprint of ref 26 and useful discussions. We also thank Kevos Spartalian, Robert Ditchfield, and Robert Cantor for helpful discussions and Norma Leonida and John Goldman for technical assistance. We are grateful for a Bristol-Myers Co. Grant from the Research Corp. and for USDA Competitive Research Grant No. 87-CRCR-1-2485, which supported this research.

Contribution from the Department of Chemistry,
University of Texas, Austin, Texas 78712

Binding of Pyridine and Benzimidazole to a Cadmium "Expanded Porphyrin": Solution and X-ray Structural Studies

Jonathan L. Sessler,* Toshiaki Murai, and Vincent Lynch

Received October 5, 1988

The characterization by X-ray diffraction analysis of a six-coordinate pentagonal-pyramidal cadmium(II) cationic complex **4b** derived from a novel aromatic 22-π-electron pentadentate "expanded porphyrin" ligand (**2**) is described. $Cd(C_{32}H_{34}N_5)(C_7H_6N_2)NO_3 \cdot CHCl_3$ crystallizes in the triclinic space group $P\bar{1}$ (No. 2) in a cell of dimensions a = 11.276 (4) Å, b = 12.845 (3) Å, c = 14.913 (4) Å, α = 84.82 (2)°, β = 69.57 (2)°, γ = 85.84 (2)°, and V = 2014 (1) Å^3 with Z = 2. The structure was solved by the heavy-atom method and refined by full-matrix least squares in blocks of 253 and 287 parameters. The final R = 0.0781 and R_w = 0.114 from 3294 reflections with $F_o > 6(\sigma(F_o))$. The X-ray structure reveals the five central donor atoms of the macrocycle to be coordinated to the cadmium(II) cation, which in turn lies 0.334 (2) Å above the mean plane of the macrocycle and is further ligated by an apical benzimidazole ligand. As is true in the corresponding pentagonal-bipyramidal bis(pyridine) adduct **5a**, the X-ray structure of cation **4b** indicates the macrocyclic ligand to be nearly planar (maximum deviation 0.154 (13) Å for C15) with the five donor nitrogen atoms defining a near-circular cavity with a center-to-nitrogen radius of $\simeq$2.42 Å. The crystals of **4b**(NO_3) used for the X-ray diffraction analysis were isolated from an inhomogeneous mixture of crystalline and noncrystalline material obtained following treatment of the sp^3 form of the ligand (**1**) with $Cd(NO_3)_2 \cdot 4H_2O$ and subsequent purification on Sephadex. The proton NMR spectrum in $CDCl_3$ of this bulk material is essentially identical with that of the pure five-coordinate complex **3** prepared independently but showed the presence of a broad feature at ca. 6.4 ppm and two sharper peaks at 6.81 and 7.27 ppm ascribable to the bound benzimidazole ligand. These diagnostic ligand features are reproduced upon titrating the pure five-coordinate complex **3** with roughly $^3/_5$ equiv of benzimidazole. This finding suggests that the bulk material from which crystals of **4b**(NO_3) were isolated consists of a mixture of crystalline and noncrystalline six- and five-coordinate species and supports the hypothesis that the bound benzimidazole found in cation **4b** is derived from degradative side reactions associated with the metal insertion and accompanying ligand oxidation. From these titrations the values for the sequential formation constants (K_1 and K_2) for the binding of the first and second equivalents of benzimidazole to the five-coordinate cationic complex **3** were determined to be 1.8 × 10^4 and 13 M^{-1}, respectively. For the complexation of pyridine to **3**(NO_3), K_1 and K_1K_2 values of 1.6 M^{-1} and 315 M^{-2}, respectively, were determined from similar ^{1}H NMR titrations. These results indicate that in benzimidazole-containing chloroform solutions an extended concentration range exists wherein the *pentagonal-pyramidal* complex **4b** is the primary cadmium-containing species, whereas in the presence of pyridine it is either the unligated complex **3** or the coordinatively saturated *pentagonal-bipyramidal* species **5a** that will dominate in solution.

Although the porphyrins and related tetrapyrrolic compounds remain among the most widely studied of all known macrocycles,[1] relatively little effort has been devoted to the development of larger conjugated pyrrole-containing systems.[2-12] Large, or "expanded", porphyrin-like systems, however, are of interest for several reasons: They could serve as possible aromatic analogues of the better

(1) *The Porphyrins*; Dolphin, D., Ed.; Academic Press: New York, 1978–1979; Vol. I–VII.
(2) (a) Day, V. W.; Marks, T. J.; Wachter, W. A. *J. Am. Chem. Soc.* **1975**, *97*, 4519–4527. (b) Marks, T. J.; Stojakovic, D. R. *J. Am. Chem. Soc.* **1978**, *100*, 1695–1705. (c) Cuellar, E. A.; Marks, T. J. *Inorg. Chem.* **1981**, *20*, 3766–3770.
(3) Bauer, V. J.; Clive, D. R.; Dolphin, D.; Paine, J. B., III; Harris, F. L.; King, M. M.; Loder, J.; Wang, S.-W. C.; Woodward, R. B. *J. Am. Chem. Soc.* **1983**, *105*, 6429–6436. To date only tetracoordinated metal complexes have been prepared from these potentially pentadentate ligands.
(4) Broadhurst, M. J.; Grigg, R.; Johnson, A. W. *J. Chem. Soc., Perkin Trans. 1* **1972**, *2111*–2116.
(5) Broadhurst, M. J.; Grigg, R.; Johnson, A. W. *J. Chem. Soc. D* **1969**, 23–24. Broadhurst, M. J.; Grigg, R.; Johnson, A. W. *J. Chem. Soc. D* **1969**, 1480–1482. Broadhurst, M. J.; Grigg, R.; Johnson, A. W. *J. Chem. Soc. D* **1970**, 807–809.
(6) (a) Berger, R. A.; LeGoff, E. *Tetrahedron Lett.* **1978**, 4225–4228. (b) LeGoff, E.; Weaver, O. G. *J. Org. Chem.* **1987**, *52*, 710–711.
(7) (a) Rexhausen, H.; Gossauer, A. *J. Chem. Soc., Chem. Commun.* **1983**, 275. (b) Gossauer, A. *Bull. Soc. Chim. Belg.* **1983**, *92*, 793–795.
(8) (a) Gosmann, M.; Franck, B. *Angew. Chem.* **1986**, *98*, 1107–1108; *Angew. Chem., Int. Ed. Engl.* **1986**, *25*, 1100–1101. (b) Knübel, G.; Franck, B. *Angew. Chem.* **1988**, *100*, 1203–1205; *Angew. Chem., Int. Ed. Engl.* **1988**, *27*, 1170–1172.
(9) For examples of porphyrin-like systems with *smaller* central cavities see: (a) Vogel, E.; Kocher, M.; Schmickler, H.; Lex, J. *Angew. Chem.* **1986**, *98*, 262–263; *Angew. Chem., Int. Ed. Engl.* **1986**, *25*, 257–258. (b) Vogel, E.; Balci, M.; Pramod, K.; Koch, P.; Lex. J.; Ermer, O. *Angew. Chem.* **1987**, *99*, 909–912; *Angew. Chem., Int. Ed. Engl.* **1987**, *26*, 928–931.
(10) For examples of large nonaromatic pyrrole-containing macrocycles see: (a) Acholla, F. V.; Mertes, K. B. *Tetrahedron Lett.* **1984**, 3269–3270. (b) Acholla, F. V.; Takusagawa, F.; Mertes, K. B. *J. Am. Chem. Soc.* **1985**, *107*, 6902–6908. (c) Adams, H.; Bailey, N. A.; Fenton, D. A.; Moss, S.; Rodriguez, de Barbarin, C. O.; Jones, G. *J. Chem. Soc., Dalton Trans.* **1986**, 693–699. (d) Fenton, D. E.; Moody, R. *J. Chem. Soc., Dalton Trans.* **1987**, 219–220.
(11) Sessler, J. L.; Murai, T.; Lynch, V.; Cyr, M. *J. Am. Chem. Soc.* **1988**, *110*, 5586–5588.

0020-1669/89/1328-1333$01.50/0

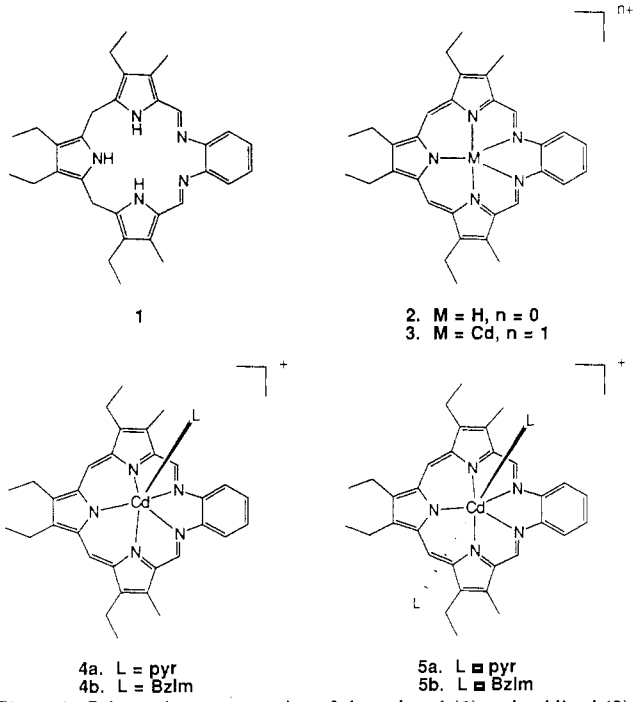

Figure 1. Schematic representation of the reduced (**1**) and oxidized (**2**) forms of the free-base porphyrin-like macrocycle and representative five-, six-, and seven-coordinate cadmium complexes (**3–5**) derived from this "expanded porphyrin".

studied porphyrins[2-8] or serve as potential biomimetic models for these or other naturally occurring pyrrole-containing systems.[13,14] In addition, large pyrrole-containing systems offer exciting possibilities as novel metal-binding macrocycles.[2,9-12,15] For instance, suitably designed systems could act as versatile ligands capable of binding larger metal cations and/or stabilizing coordination geometries[2,16] higher than those routinely accommodated within the normally tetradentate ca. 2.0 Å radius porphyrin core.[17] The resulting complexes could have important application in the area of heavy-metal chelation therapy or as new vehicles for extending the range and scope of coordination chemistry.[15,18] In recent years a number of potentially pentadentate polypyrrolic aromatic systems, including the sapphyrins,[3,4] oxosapphyrins,[5] smaragdyrins,[3,4] platyrins,[6] and pentaphyrin,[7] have been prepared and studied as their metal-free forms. For the most part, however, little or no information is available for the corresponding metalated forms. Indeed, at the outset of this work,[11] the uranyl complex of superphthalocyanine was the only metal-containing pentapyrrolic system to be prepared and characterized structurally.[2] Unfortunately, the superphthalocyanine system is apparently not capable of existence in either its free base or other metal-containing forms.[2] Thus, prior to the present work, no versatile, structurally characterized, pentadentate aromatic ligands were available,[11] although a number of aza-crown and nonaromatic pyridine-derived pentadentate systems have previously been reported.[12,19,20] Our goals

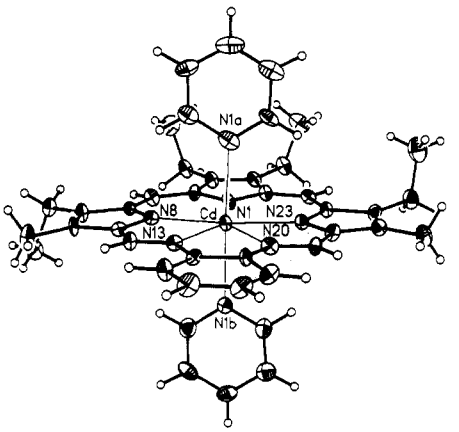

Figure 2. View of the cation **5a** showing pyridine and macrocycle coordination to Cd. Ellipsoids are scaled to the 30% probability level. The cadmium(II) cation lies in the plane of the nearly planar macrocycle (maximum deviation from planarity 0.10 (1) Å). Relevant Cd–N bond lengths (Å) are as follows: 2.418 (7), N1; 2.268 (8), N8; 2.505 (7), N13; 2.521 (7), N20; 2.248 (8), N23; 2.438 (14), N1a; 2.473 (12), N1b. Selected N–Cd–N bond angles (deg) are as follows: 78.9 (2), N1–Cd–N8; 80.2 (3), N1–Cd–N23; 68.4 (2), N8–Cd–N13; 64.4 (2), N13–Cd–N20; 68.2 (3), N20–Cd–N23; 176.1 (4), N1a–Cd–N1b. For further structural details, see ref 11.

were therefore to develop a new class of pyrrole-derived aromatic "expanded porphyrins" capable of binding a variety of metal cations and stabilizing a range of unusual coordination geometries. We have recently communicated the synthesis of **2**,[11] an unprecedented porphyrin-like monoanionic aromatic *pentadentate* ligand,[18] and the structure of its *seven-coordinate* cadmium(II) bis(pyridine) *pentagonal-bipyramidal* complex **5a**. Due to the importance of cadmium complexes in possible chelation-based therapeutic applications[21,22] and as potential structural probes for natural metalloproteins (e.g. employing ^{113}Cd NMR spectroscopy),[23] we sought to investigate further the coordination properties of the cadmium-containing "expanded porphyrin" system. We now wish to report the characterization by single-crystal X-ray diffraction analysis of the monoligated *six-coordinate* cadmium(II) benzimidazole *pentagonal-pyramidal* cationic complex **4b** corresponding formally to a coordinatively unsaturated analogue of **5a**. To the best of our knowledge the present report, which includes the results of solution base-binding (K_{eq}) studies for both pyridine (py) and benzimidazole (BzIm), constitutes the first structurally documented instance wherein the same macrocyclic ligand has

(12) For a general review of pentadentate ligand systems and for an intercomparison between those containing one or more aromatic subunits (e.g. **3**(NO_3)) and simple aza-crown compounds, see: Sessler, J. L.; Cyr, M.; Murai, T. *Comments Inorg. Chem.* **1988**, *7*, 333–350.

(13) Stark, W. M.; Baker, M. G.; Raithby, P. R.; Leeper, F. J.; Battersby, A. R. *J. Chem. Soc., Chem. Commun.* **1985**, 1294.

(14) Sessler, J. L.; Johnson, M. R.; Lynch, V. *J. Org. Chem.* **1987**, *52*, 4394–4397.

(15) Sessler, J. L.; Johnson, M. R.; Lynch, V.; Murai, T. *J. Coord. Chem.* **1988**, *18*, 99–104.

(16) Sessler, J. L.; Murai, T.; Hemmi, G. Submitted for publication in *Inorg. Chem.*

(17) Hoard, J. L. In *Porphyrins and Metalloporphyrins*; Smith, K., Ed.; Elsevier: Amsterdam, 1975; Chapter 8.

(18) *Chem. Eng. News* **1988**, *66* (Aug 8), 26–27.

(19) For reviews see: (a) Drew, M. G. B. *Prog. Inorg. Chem.* **1977**, *23*, 67–210. (b) Melson, G. A. In *Coordination Chemistry of Macrocyclic Compounds*; Melson, G. A., Ed.; Plenum: New York, 1979; Chapter 1. (c) Curtis, N. F. In *Coordination Chemistry of Macrocyclic Compounds*; Melson, G. A., Ed.; Plenum: New York, 1979; Chapter 4. (d) Nelson, S. M. *Pure Appl. Chem.* **1980**, *52*, 2461–2476. (e) Lindoy, L. F. In *Synthesis of Macrocycles*; Izatt, R. M., Christensen, J. J., Eds.; Wiley: New York, 1987; Chapter 2. (f) Newkome, G. R.; Gupta, V. K.; Sauer, J. D. In *Heterocyclic Chemistry*; Newkome, G. R., Ed.; Wiley: New York, 1984; Vol. 14, Chapter 3. (g) De Sousa, M.; Rest, A. J. *Adv. Inorg. Chem. Radiochem.* **1978**, *21*, 1–40.

(20) For recent examples of bipyridine-derived systems and related pentadentate ligands, see: (a) Ansell, C. W. G.; Lewis, J.; Raithby, P. R.; Ramsden, J. N.; Schroder, M. *J. Chem. Soc., Chem. Commun.* **1982**, 564–547. (b) Lewis, J.; O'Donoghue, T. D.; Raithby, P. R. *J. Chem. Soc., Dalton Trans.* **1980**, 1383–1389. (c) Constable, E. C.; Chung, L.-Y.; Lewis, J.; Raithby, P. R. *J. Chem. Soc., Chem. Commun.* **1986**, 1719–1720. (d) Constable, E. C.; Holmes, J. M.; McQueen, R. C. S. *J. Chem. Soc., Dalton Trans.* **1987**, 5–8. (e) Constable, E. C.; Doyle, M. J.; Healy, J.; Raithby, P. R. *J. Chem. Soc., Chem. Commun.* **1988**, 1262–1264.

(21) Ochai, E.-I. *Bioinorganic Chemistry*; Allyn and Bacon: Boston, 1977; pp 475–476.

(22) Klaasen, C. D. In *The Pharmacological Basis of Therapeutics*, 6th ed.; Gilman, A. G., Goodman, L. S., Gilman, A., Eds.; Macmillan: New York, 1980; Chapter 69, pp 1632–1633.

(23) For recent reviews see: (a) Summers, M. F. *Coord. Chem. Rev.* **1988**, *86*, 43–134. (b) Ellis, P. D. *Science* **1983**, *221*, 1141–1146. (c) Ellis, P. D. In *The Multinuclear Approach to NMR Spectroscopy*; Lambert, J. B., Riddell, F. G., Eds.; D. Reidel: Amsterdam, 1983; pp 457–523.

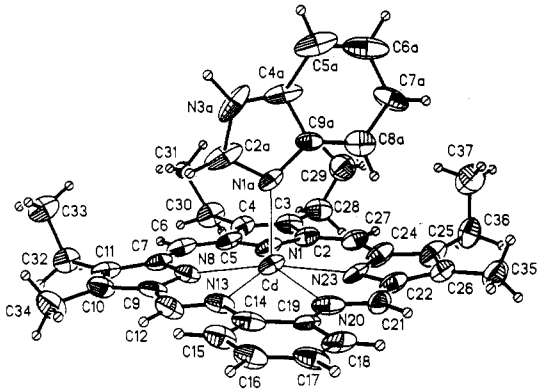

Figure 3. View of cation **4b** showing the atom-labeling scheme. Thermal ellipsoids are drawn to the 30% probability level. Relevant Cd–N bond lengths (Å) are as follows: N1, 2.462 (13); N8, 2.254 (9); N13, 2.535 (13); N20, 2.526 (12); N23, 2.298 (11); N1a, 2.310 (9). Selected N–Cd–N bond angles (deg) are as follows: 78.3 (4), N1–Cd–N8; 67.8 (4), N8–Cd–N13; 64.1 (4), N13–Cd–N20; 67.3 (4), N20–Cd–N23. N1a–Cd–macrocycle N angles range from 93.7 (4) to 100.4 (3)°. The Cd atom lies 0.338 (4) Å out of the plane defined by nitrogens N1, N8, N13, N20, and N23. The coordinated BzIm ligand is oriented nearly perpendicular to the macrocycle (dihedral angle of 86.3 (3)°) and lies over the pyrrole ring defined by C22, N23, C24, C25, and C26. The nitrate counteranion (not shown) is not coordinated to the Cd atom.

been used to support these two rare, but not unknown,[19] coordination geometries about the same metal cation.[24]

Results and Discussion

Synthesis and Structure. Treatment of the reduced, sp^3 form of the macrocycle (**1**)[14] with cadmium chloride or cadmium nitrate in air-saturated chloroform–methanol leads in both cases to the formation of green solutions. Following chromatographic purification on silica gel and recrystallization from chloroform–hexane, the five-coordinate "expanded porphyrin" chloride and nitrate complexes **3**(Cl) and **3**(NO_3) are obtained in analytically pure form (as the semihydrates) in roughly 25% yield. When, however, the metal-insertion procedure is carried out (with cadmium nitrate) under reaction and purification conditions identical with those described above, with the exception that chromatography is effected on Sephadex, a mixture of crystalline and noncrystalline green solids is obtained. Treatment of this apparently inhomogeneous bulk material, which fails to give an analysis as a pure five-coordinate complex, with excess pyridine and recrystallization from chloroform–hexanes produce the bis(pyridine) complex **5a**(NO_3) as dark green crystals in essentially quantitative yield. As communicated earlier,[11] an X-ray crystal diffraction analysis served to confirm the pentagonal-bipyramidal coordination geometry postulated for this bisligated seven-coordinate complex and the planar pentadentate nature of the porphyrin-like macrocyclic ligand **2** (cf. Figure 2). Left undetermined, however, was the exact nature of the intermediate cadmium-containing material.

As a first step toward determining the nature of the above intermediate product, a single crystal was isolated from the inhomogeneous solid mixture and subjected to an X-ray diffraction analysis. The structure so obtained (Figure 3) was quite unexpected: It revealed a six-coordinate pentagonal-pyramidal cadmium(II) complex (**4b**(NO_3)) wherein one of the two possible axial ligation sites is occupied by a bound benzimidazole (BzIm) with the nitrate counteranion not being coordinated to the central Cd atom. The five donor nitrogens of the pentadentate "expanded porphyrin" macrocycle then serve to complete the coordination sphere about cadmium. As shown in Figure 3, the five donor atoms of the ligand are bound to the Cd atom, which lies out of the plane of the macrocycle, being displaced by 0.338 (4) Å from the N_5 donor plane toward the coordinated nitrogen of the benzimidazole ligand. This out-of-plane distance, which is similar to that seen in CdTPP(dioxane)$_2$[25] (0.32 Å)[26] (but smaller than that observed in CdTPP[27]), is in marked contrast to that observed for the corresponding bis(pyridine) pentagonal-bipyramidal adduct **5a**(NO_3).[11] In this earlier structure, the cadmium(II) cation was found to lie essentially within the plane of the macrocycle (cf. Figure 2). Cation **4b** further differs from **5a** in that, within the crystal lattice, two molecules stack on one another in a face-to-face fashion, being separated by van der Waals distances of ca. 3.38 Å (cf. Figure 1 of the supplementary material accompanying this paper). As a result, the alkyl groups in any given molecule are all displaced to the BzIm-bearing side of the macrocyclic plane. In common with the bis(pyridine) structure,[11] however, in cation **4b** the sp^2 atoms of the macrocycle are all essentially planar, with the maximum deviation from planarity (0.154 (13) Å) being found for C11. Also in common with complex **5a**(NO_3), the five ligand nitrogens define a near-circular binding cavity with a center-to-nitrogen radius of ca. 2.42 Å, which is roughly 20% larger than that found in metalloporphyrins (cf. Figure 2 of the supplementary material accompanying this paper).[17]

The above structural results support the original formulation of **2** as a large 22-π-electron (or benzannelated 18-π-electron) aromatic porphyrin-like ligand.[28] They also clearly demonstrate that this "expanded porphyrin" is capable of supporting more than one kind of "unusual" coordination geometry about cadmium.

The above structural results also provide some insight into the nature of the inhomogeneous cadmium-containing intermediate obtained following metal insertion and Sephadex-based purification: At least a portion of this material consists of the six-coordinate BzIm-ligated complex **4b**(NO_3). Although it is certainly plausible to postulate that the coordinated BzIm in cation **4b** derives from ligand-degradation reactions associated with metal insertion and accompanying oxidation (presumably involving electrophilic aromatic deacylation of an tripyrrane α-carbon and subsequent condensation with *o*-phenylenediamine), the observation of this six-coordinate species does not establish unambiguously that such BzIm coordination is chemically reasonable. This point is of particular interest since, in the presence of excess pyridine, it is the bisligated seven-coordinate cationic species **5a** that is favored in the solid state. Thus, we considered it of paramount importance to determine the solution binding properties of **3**(NO_3) in the presence of both benzimidazole and pyridine. Our objective was not only to probe the ligation differences (if any) of these two axial bases but also to define further the nature of the intermediate inhomogeneous solid material formed following Cd insertion and Sephadex-based purification, testing in particular the reasonable assumption that this material consists of a mixture of the five- and six-coordinate cations **3** and **4b**.

Equilibria of Interest. For a rigorously five-coordinate starting cadmium complex, such as that represented schematically by structure **3**, where neither the counteranion nor adventitious ligands serve to occupy an apical coordination site, base binding can be considered to occur in accord with eq 1 and 2. Under conditions

(24) Interestingly, pentagonal-pyramidal and pentagonal-bipyramidal geometries have been observed in two very closely related pentadentate macrocyclic Schiff base ligands that differ only in the size of the ring (16 vs 17 atoms); see: (a) Nelson, S. M.; McFall, S. G.; Drew, M. G. B.; Othman, A. H. *J. Chem. Soc., Chem. Commun.* **1977**, 167–168. (b) Drew, M. G. B.; McFall, S. G.; Nelson, S. M. *J. Chem. Soc., Dalton Trans.* **1977**, 575–581.

(25) OEP = octaethylporphyrin, TPP = tetraphenylporphyrin, and PPIXDME = protoporphyrin IX dimethyl ester, with the prefixes H_2 and Cd referring to the free-base and cadmium(II) forms, respectively; BzIm = benzimidazole; py = pyridine.

(26) Rodesiler, P. F.; Griffith, E. H.; Ellis, P. D.; Amma, E. L. *J. Chem. Soc., Chem. Commun.* **1980**, 492–493.

(27) Hazell, A. *Acta Crystallogr.* **1986**, *C42*, 296–299.

(28) The "expanded porphyrin" **2** and its derivatives can be formulated either as a benzannelated [18]annulene or as an overall 22-π-electron aromatic system. On the basis of preliminary molecular orbital calculations, and spectral comparisons to an 18-π-electron macrocyclic analogue of **3**(NO_3) derived from diaminomaleionitrile, for which a lowest energy Q-type transition of 692 nm is observed, we currently favor the 22-π-electron formulation: Hemmi, G.; Krull, K., Cyr, M., Sessler, J. L. Unpublished results.

$$L + B \rightleftarrows LB \qquad K_1 = [LB]/[L][B] \qquad (1)$$

$$LB + B \rightleftarrows LB_2 \qquad K_2 = [LB_2]/[LB][B] \qquad (2)$$

$$L + 2B \rightleftarrows LB_2 \qquad K_1K_2 = [LB_2]/[L][B]^2 \qquad (3)$$

where $K_1 \geq K_2$, these processes can be considered to occur sequentially, giving first a monoligated, presumably pentagonal-pyramidal six-coordinate species (such as **4b**), followed by a coordinatively saturated bisligated pentagonal-bipyramidal product akin to **5a**. Where, however, $K_2 \gg K_1$, this stepwise conceptual approach is invalid. Under these conditions, it becomes easier to analyze the base binding in terms of direct formation of the bisligated material as shown in eq 3. In the context of the present study, therefore, the problem becomes one of finding a solution-based analytical method that will allow changes associated with mono- and bisligation to be probed and using the accompanying changes to determine as appropriate K_1, K_2, or K_1K_2.

Optical Spectroscopy. Optical spectroscopy often provides a convenient means of determining base-binding constants.[29] In the case of CdTPP,[25] for instance, Miller and Dorough[30] determined a value for the binding of a single pyridine axial ligand to the unligated four-coordinate starting metalloporphyrin in benzene at 29.9 °C (K_1) of roughly 2700 M^{-1} by monitoring the changes associated with the two low-energy Q bands of the absorption spectrum. Interestingly, these[30] and later workers[31] obtained no evidence for the formation of a bisligated $CdTPP(py)_2$[25] species. Thus, although a pseudooctahedral coordination geometry is defined in the solid state by the weakly bound axial ligands of $CdTPP(dioxane)_2$,[26] there is no evidence that such a structure is attained in pyridine-containing benzene solution.

The optical spectrum of purifined $3(NO_3)$ (cf. Figure 3 of the supplementary material accompanying this paper) bears some elements in common with those of cadmium porphyrins.[30-34] For instance, complex $3(NO_3)$ in $CHCl_3$ displays a strong Soret-like high-energy transition at 425 nm (ϵ = 82 800), which is considerably less intense than that seen in cadmium porphyrins (e.g. CdOEP:[25] λ_{max} ($CHCl_3$/MeOH, 19/1 v/v) = 406 nm, ϵ = 272 000).[35] This complex also displays exceptionally strong flanking N- and Q-like bands at higher and lower energy. The lowest energy Q-like band (λ_{max} = 770 nm, ϵ = 49 800) is particularly noteworthy: It is shifted to the red by ca. 200 nm and is almost a factor of 4 more intense than the lowest energy Q-type transition seen in typical cadmium porphyrins (e.g. CdOEP: λ_{max} ($CHCl_3$/MeOH, 19/1 v/v) = 571 nm, ϵ = 15 400).[35] We consider such behavior to be reflective of the larger delocalized aromatic system present in the overall 22-π-electron[28] porphyrin-like macrocycles than in the 18-π-electron porphyrins. Unfortunately, optical spectroscopy proved to be an ineffective means of determining the axial ligation properties of cation **3**. For instance, addition of excess pyridine to a solution of $3(NO_3)$ in $CHCl_3$ caused only a ca. 1.5-nm red shift in the Soret-like band and a 3.5-nm blue shift of the lowest energy Q-type band. (Similar insignificant changes are also observed upon BzIm addition.) Thus, at least in the case of the cadmium complexes, the optical properties of the "expanded porphyrin" system appear to be largely determined by the overall macrocyclic skeleton and relatively insensitive to changes in the electron environment of the bound cation.

Proton NMR Spectroscopy. Cadmium(II) complexes of **2** are diamagnetic and hence readily susceptible to study by ^1H NMR methods. As shown in Figure 4, the ^1H NMR spectrum of $3(NO_3)$

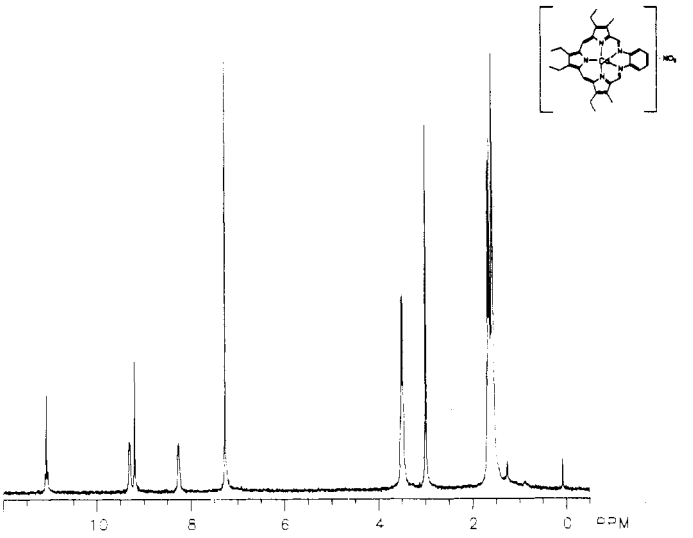

Figure 4. ^1H NMR spectrum of complex $3(NO_3)$ in $CDCl_3$. The signals at 1.5 and 7.26 ppm represent residual water and solvent peaks, respectively.

shows general features that are typical of those expected for a large aromatic pyrrole-containing macrocycle.[36] As compared to the spectrum for the sp^3 form of the ligand (**1**),[14] for instance, the alkyl and aromatic peaks are substantially shifted to lower field. Moreover, two sharp "meso"-like signals are observed at 9.2 and 11.1 ppm in compounds **2–5**. On the basis of NOE studies, these are assigned to the bridging sp^2-hybridized methine (CH=C) and imine (CH=N) protons, respectively. Thus, the bridging methine protons of **2–5** resonate at ca. 5 ppm lower field than the corresponding methylene protons in the original sp^3 form of the ligand (**1**)[14] and fall in a chemical shift region that is roughly 1 ppm *upfield* from those of typical β-alkyl-substituted free-base and cadmium porphyrins (e.g.: H_2OEP,[25,36] $\delta \cong 10.2$; CdOEP,[25,36] $\delta \cong 10.0$). When they are taken together, these observations suggest that the "expanded porphyrin" compounds reported here are accurately formulated as delocalized π systems but that the overall degree of aromaticity may be lower than that of the porphyrins.

The ^1H NMR spectra of $3(NO_3)$ and the crude material from which the crystals of cation **4b** were obtained are almost identical except that in the latter a small broad signal at ca. 6.4 ppm and two sharper, more pronounced peaks at 6.81 and 7.27 ppm are observed (cf. Figure 4 of the supplementary material accompanying this paper). These features are assigned as signals arising from bound BzIm present in cation **4b**, even though the carbon-bound protons of free BzIm in $CDCl_3$ resonate at 7.25 (m, 2 H), 7.75 (m, 2 H), and 8.41 (s, 1 H) ppm.[37] This is because the addition of roughly $^3/_5$ equiv of BzIm to purified $3(NO_3)$ reproduces precisely those additional spectral features characteristic of the crude material from which cation **4b** was isolated (cf. Figure 5 of the supplementary material accompanying this paper). This dramatic result provides support for the structural assignment of cation **4b** made on the basis of X-ray diffraction analysis. It also confirms qualitatively the original supposition that the inhomogeneous material isolated after Cd insertion and Sephadex purification does indeed involve an admixture of five- and six-coordinated species (i.e. $3(NO_3)$ and $4b(NO_3)$).

For quantitative K_{eq} determinations it proved easiest to monitor the changes associated with the "meso"-like imine (CH=N) signals. Here, sharp peaks, indicative of fast ligand exchange,[29,38] and reasonably large changes in chemical shift were observed (Figure 5). In addition, no interfering BzIm-based resonances

(29) Drago, R. S. *Physical Methods in Chemistry*; W. B. Saunders: Philadelphia, 1977; Chapter 5.
(30) Miller, J. R.; Dorough, G. D. *J. Am. Chem. Soc.* **1952**, *74*, 3977–3981.
(31) Kirksey, C. H.; Hambright, P. *Inorg. Chem.* **1970**, *9*, 958–960.
(32) For general discussions see: Gouterman, M. In ref 1, Vol. III, Chapter 1.
(33) Dorough, G. D.; Miller, J. R. *J. Am. Chem. Soc.* **1951**, *73*, 4315–4320.
(34) Edwards, L.; Dolphin, D. H.; Gouterman, M.; Adler, A. D. *J. Mol. Spectrosc.* **1971**, *38*, 16–32.
(35) Johnson, M. R.; Cyr, M.; Sessler, J. L. Unpublished results.
(36) (a) Scheer, H.; Katz, J. J. In ref 17, Chapter 10. (b) Janson, T. R.; Katz, J. J. In ref 1, Vol. IV, Chapter 1.
(37) *Aldrich Library of NMR Spectroscopy*, 2nd Ed.; Pouchert, C. J., Ed.; Aldrich: Milwaukee, 1983; Vol. 2, p 558.
(38) Connors, K. A. *Binding Constants*; Wiley: New York, 1987.

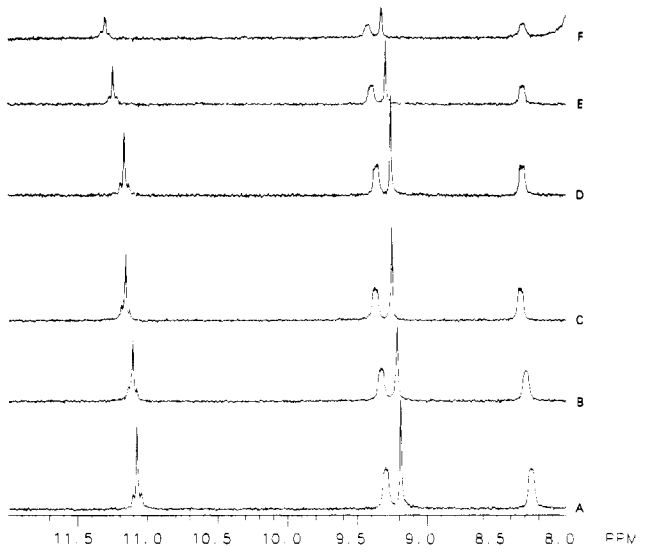

Figure 5. ^{1}H NMR spectral titration of $3(NO_3)$ (initially 6.85×10^{-3} M in $CDCl_3$) with increasing quantities of BzIm showing changes occurring in the downfield region. The [BzIm]/[$3(NO_3)$] ratios are 0, 0.2, 0.6, 2.8, 10, and 40 for traces A–F, respectively, where [BzIm] and [$3(NO_3)$] represent the total molar concentrations of added benzimidazole and starting five-coordinate complex $3(NO_3)$.

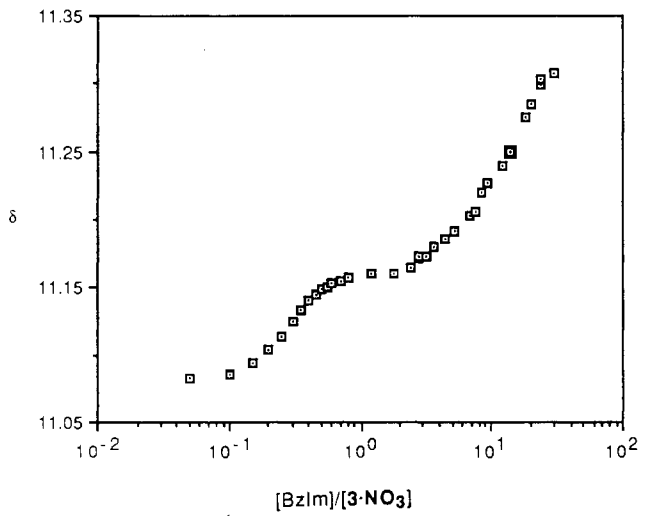

Figure 6. Changes in the ^{1}H NMR chemical shift of the imine CH signal for $3(NO_3)$ plotted as a function of increasing [BzIm]. The terms [BzIm] and [$3(NO_3)$] represent the total molar concentrations of added benzimidazole and starting five-coordinate complex $3(NO_3)$.

are found in this region. In Figure 6 the changes in chemical shift for these imine protons of complex $3(NO_3)$ are plotted as a function of added BzIm. The resulting titration curve shows that, at least for this base, axial ligation can be considered as occurring in two essentially independent stepwise binding processes. Standard analysis[38] of the data at both very low and very high conversion gave values of $K_1 = (1.8 \pm 0.2) \times 10^4$ and $K_2 = 13 \pm 3$. (Cf. Experimental Section and the supplementary material for calculational details.)

Just as was the case for BzIm, addition of pyridine to the five-coordinate complex $3(NO_3)$ gave rise to easily detected and well-defined changes in the chemical shift of the "meso"-like imine (CH=N) signals (Figure 7). In marked contrast to the results obtained with BzIm, however, ligation in this case cannot be considered to be occurring in a discrete stepwise manner. This is quite apparent from an inspection of Figure 8, in which the changes in chemical shift for the imine protons of complex $3(NO_3)$ are plotted as a function of increasing pyridine concentration. Analysis of this binding isotherm using standard methods[38] then gave values of $K_1 \cong 1.6$ M^{-1} and $K_1K_2 = 315 \pm 30$ M^{-2}. (Calculational details are provided in the Experimental Section and in the supplementary material accompanying this paper.)

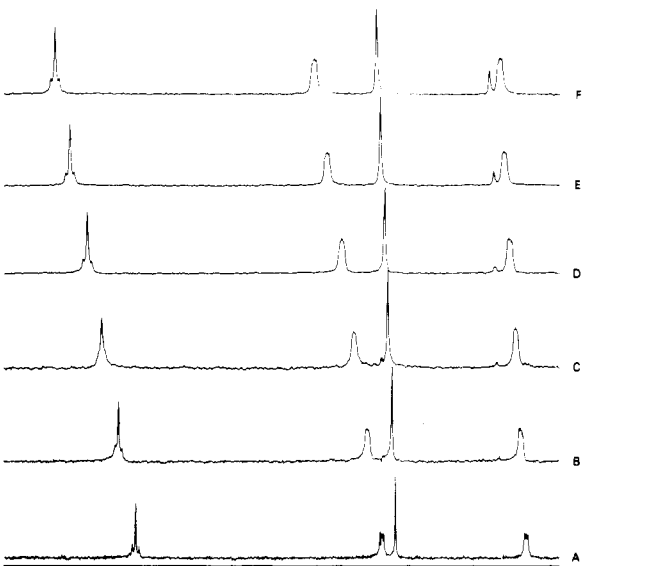

Figure 7. ^{1}H NMR spectral titration of $3(NO_3)$ (initially 6.66×10^{-3} M in $CDCl_3$) with increasing quantities of pyridine showing changes occurring in the downfield region. The [pyridine]/[$3(NO_3)$] ratios are 0, 5, 10, 14, 20, and 40 for traces A–F, respectively.

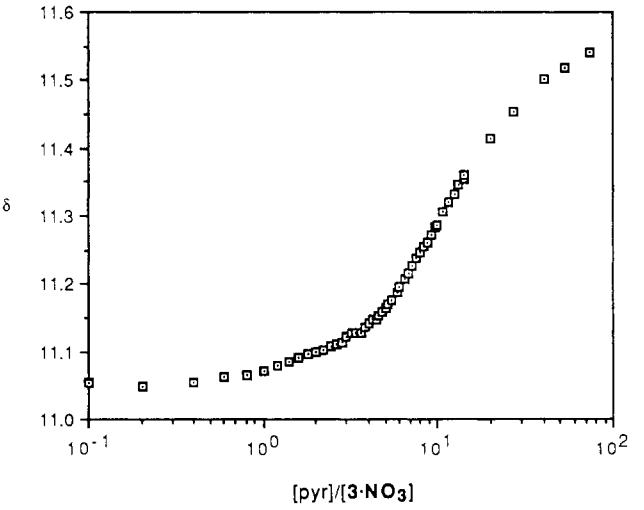

Figure 8. Changes in the ^{1}H NMR chemical shift of the imine CH signal for $3(NO_3)$ as a function of increasing pyridine concentration. The terms [pyridine] and [$3(NO_3)$] represent the total molar concentrations of added pyridine and starting five-coordinate complex $3(NO_3)$.

The above K_1 and K_2 (or K_1K_2) values are predicated on the assumption that the cadmium complexes under discussion are stable with regard to demetalation and that the equilibria of eq 1 and 2 (or 3) pertain under the conditions of base binding. The first of these concerns is readily apparent: If demetalation occurs, then obviously one is not studying base binding! All control experiments, however, suggest that the cadmium complexes derived from the "expanded porphyrin" ligand are many orders of magnitude more stable than those of the considerably smaller porphyrins. In fact, demetalation does not occur even when the complexes are challenged with excess sulfide anion (which serves to demetalate CdTPP[25,35]) or sodium thiosulfate;[39] it thus appears unlikely that such a demetalation process will occur in the presence

(39) We ascribe much of this stability to kinetic factors: Direct insertion of Cd^{2+} into the preformed "expanded porphyrin" **2** does not take place at an appreciable rate. This suggests that the *kinetic* barrier is substantial for metal complexation; the same is likely to be true for decomplexation. When subject to treatment with aqueous acid, the complex $3(NO_3)$ appears to undergo hydrolysis (at the imine residues) and hence demetalation. The rate of this process, however, is strongly pH dependent, the half-life being, for instance, on the order of several hours in the presence of ca. 0.1 N HCl.

of pyridine or benzimidazole. The second concern is particularly important within the context of quantitative work: If, for instance, the starting complex **3**(NO_3) is not rigorously five-coordinate, then K_1 (and perhaps K_2 as well) would represent an axial ligand displacement reaction rather than a pure addition process as implied above. Control experiments indicate that the assumption of initial five-coordination is reasonable: Independent titrations of **3**(NO_3) with NH_4NO_3 and H_2O indicate that only modest and monotonic changes in the chemical shift of the imine (CH=N) signals take place over the course of adding ≥50 equiv of these potentially adventitious ligands.[40] This means either that "complete" binding occurs at 1:1 stoichiometry (essentially ruled out in the case of H_2O on the basis of analytical data) or that these species are poorly coordinating in $CHCl_3$ so that five-coordination pertains about cadmium; we favor the latter interpretation.

To the extent that the above assumptions are valid, the K_{eq} values obtained for BzIm and py binding *in solution* provide an accurate reflection of the coordination behavior observed *in the solid state*. For instance, at the concentrations used for the ^1H NMR titration experiments (ca. 5×10^{-3} M) complex **3**(NO_3) will be roughly 20% converted to the six-coordinate form (**4b**-(NO_3)) following the addition of only 0.2 molar equiv of BzIm and 90% converted after the addition of 1.0 molar equiv. Interestingly, even in the presence of 10 molar equiv, the resulting monoligated species **4b** will only be 35% converted to the corresponding bisligated seven-coordinate form (**5b**). Thus, for benzimidazole a large concentration range pertains *in solution*, wherein the monoligated cationic complex **4b** is the dominant species. The equilibrium data also show, however, that *in solution* it will always be either the bisligated species **5a** or unligated starting complex **3** that dominates in the presence of excess pyridine. For instance, under the conditions of the ^1H NMR titrations, complex **3**(NO_3) will be roughly 5% converted to the pentagonal-bipyramidal product **5a**(NO_3) after the addition of 3 equiv of pyridine and roughly 35% converted to this species after the addition of 10 equiv.

Both steric and electronic factors may be invoked to explain the different ligation properties for pyridine and benzimidazole. Considerable work with metalloporphyrins, particularly in the context of heme model chemistry,[41] has served to establish the stronger coordinating abilities of imidazole-type ligands relative to pyridine-type bases, an observations that is generally ascribed to the poorer π basicity of the latter systems.[41a,42] Thus, the high K_1 value (relative to pyridine) observed for BzIm binding to cation **3** comes as little surprise. What is more puzzling, however, is the observation that K_2 for this base is so low: At first glance it appears unreasonable that monoligation would be stable in the presence of this stronger π base since preferential conversion to the coordinatively saturated seven-coordinate species occurs in the presence of pyridine.[43] An inspection of the crystal structure shown in Figure 3, however, provides the basis for an explanation: The BzIm residue lies nearly perpendicular to the macrocycle in **4b** and is oriented over the pyrrole ring containing N23. As a result, H8A of the BzIm base is in close proximity to several atoms of this ring, making close contacts (Å) with N23 (2.65 (2)), C24 (2.69 (2)), and C22 (2.81 (2)). Thus, as has been well documented in the case of heme models and encumbered imidazoles,[41b,44] steric hindrance appears to be the fundamental factor favoring six-coordination in the presence of excess BzIm. Therefore, both steric and electronic effects serve to differentiate the ostensibly very different binding behaviors of BzIm and py in the present "expanded porphyrin" system. Such effects also provide inter alia a rationale for the formation and selective isolation, *in the solid state*, of complexes **4b**(NO_3) and **5a**(NO_3).

Conclusions

The pentadentate 22-π-electron porphyrin-like macrocycle is an effective and versatile ligand for cadmium(II). It is capable of supporting the formation of three rare coordination geometries for this cation, namely, pentagonal, pentagonal pyramidal, and pentagonal bipyramidal. Whereas the first of these forms is currently only inferred on the basis of analytical and solution-phase studies, the last two geometries have been characterized both in solution and in the solid state by single-crystal X-ray diffraction analyses. Our "expanded porphyrin" system thus represents, to the best of our knowledge, the first structurally documented system capable of supporting both pentagonal-pyramidal and pentagonal-bipyramidal geometries about the same central metal cation. This unique cheland also endows these cadmium complexes with several other important properties. These include an optical spectrum with an unusually low energy Q-type band and a stability with regard to demetalation which far exceeds that of the corresponding cadmium(II) porphyrins. The first of these properties suggests that the present porphyrin-like macrocycle **2** or other "expanded porphyrin" systems might find important application in the areas of photodynamic therapy or photosynthetic modeling studies where low-energy absorption properties would be beneficial.[45] The second property suggests that systems similar to those presently described might provide the basis for the development of effective chelation-based detoxification therapies for cadmium, a metal presently ranking only behind mercury and lead in toxicological importance[21] and one for which few, if any, therapies currently exist.[22] We are currently exploring these exciting possibilities.

Experimental Section

General Information. Electronic spectra were recorded on a Beckman DU-7 spectrophotometer. Proton and ^{13}C NMR spectra were obtained in $CDCl_3$ with $CHCl_3$ (δ = 7.26 ppm for ^1H and 77.0 ppm for ^{13}C) as an internal standard. Proton NMR spectra were recorded on either a Nicolet NT-360 (360 MHz) or a General Electric QE-300 (300 MHz) spectrometer. Carbon spectra were measured at 125 MHz by using the Nicolet NT-500 spectrometer. Fast atom bombardment mass spectrometry (FAB MS) was performed by using a Finnigan-MAT TSQ-70 instrument and 3-nitrobenzyl alcohol as the matrix. Elementary analyses were performed by Galbraith Laboratories. X-ray structures were solved as described below and in ref 11 and 14.

Materials. All solvents and reagents were of reagent grade quality, purchased commercially, and used without further purification. Sigma lipophilic Sephadex (LH-20-100) and Merck type 60 (230–400 mesh) silica gel were used for column chromatography. The sp^3 form of the ligand (**1**) was prepared in ≥90% yield by using the acid-catalyzed method described earlier.[14] The currently higher yield does not derive from a fundamental change in procedure but simply reflects a greater experience with this particular key reaction.

Preparation of the Free-Base "Expanded Porphyrin" 4,5,9,24-Tetraethyl-10,23-dimethyl-13,20,25,26,27-pentaazapentacyclo-[20.2.1.1^{3,6}.1^{8,11}.0^{14,19}]heptacosa-1,3,5,7,9,11(27),12,14,16,18,20,22-

(40) The addition of traces of acid causes the imine signals to shift dramatically to higher field, moving, for instance, by 0.113 ppm after the addition of 1 equiv of CF_3CO_2H; this suggests that the quantitative K_{eq} titration experiments are in fact reflecting base binding to cadmium and not simple deprotonation of an adventitiously protonated metal complex.

(41) For general discussions see: (a) Ellis, P. E., Jr.; Linard, J. E.; Szymanski, T.; Jones, R. D.; Budge, J. R.; Basolo, F. *J. Am. Chem. Soc.* **1980**, *102*, 1889–1896. (b) Brault, D.; Rougee, M. *Biochemistry* **1974**, *13*, 4591–4597. (c) Collman, J. P.; Brauman, J. I.; Doxsee, K. M.; Halbert, T. R.; Bunnenberg, E.; Linder, R. E.; LaMar, G. N.; Del Gaudio, J.; Lang, G.; Spartalian, K. *J. Am. Chem. Soc.* **1980**, *102*, 4182–4192. (d) Traylor, T. G. *Acc. Chem. Res.* **1981**, *14*, 102–109.

(42) (a) Collman, J. P.; Brauman, J. I.; Doxsee, K. M.; Sessler, J. L.; Morris, R. M.; Gibson, Q. H. *Inorg. Chem.* **1983**, *22*, 1427–1432.

(43) We remain puzzled as to why K_2 is larger than K_1 for pyridine binding. It is possible that such behavior reflects the presence of a "cooperative steric effect" wherein the complexation of a single pyridine unit serves to "flatten" the molecule upon monoligation, thus facilitating the binding of a second base; we are grateful to Prof. Daryle Busch for suggesting this possible explanation.

(44) See for instance: (a) Collman, J. P.; Reed, C. A. *J. Am. Chem. Soc.* **1973**, *95*, 2048–2049. (b) Wagner, G. C.; Kassner, R. J. *Biochim. Biophys. Acta* **1975**, *392*, 319–327. (c) See also ref 41b–d.

(45) Quantitative photochemical studies indicate that, following photoexcitation at 350 nm, the excited triplet of the cation **3** in MeOH is formed in roughly 90% quantum yield. In the absence of oxygen, the observed triplet lifetime is 55 μs; in the presence of air, the triplet state is quenched completely, producing singlet oxygen in 69% total quantum yield: Harriman, T.; Maiya, B. G.; Murai, T.; Hemmi, G.; Sessler, J. L.; Mallouk, T. E. *J. Chem. Soc., Chem. Commun.*, in press.

(25),23-tridecaene (2). Macrocycle **1**[14] (50 mg, 0.1 mmol) was stirred in methanol–chloroform (150 mL, 2/1 v/v) in the presence of *N,N,N',N'*-tetramethyl-1,8-naphthalenediamine ("Proton Sponge") for 1 day at room temperature. The reaction mixture was then poured into ice water. The organic layer was separated and washed with aqueous ammonium chloride solution and then brine. Following concentration on a rotary evaporator, the crude material was purified by chromatography on Sephadex using first pure chloroform and then chloroform–methanol (10/1 v/v) as eluents. After several faster red bands were discarded, a dark green band was collected, concentrated in vacuo, and recrystallized from chloroform–*n*-hexane to give the sp^2 form of the ligand as a dark green powder in yields ranging from 3 to 12% with the better yields only being obtained on rare occasions. ^{1}H NMR ($CDCl_3$): δ 0.90 (1 H, br s, NH), 1.6–1.8 (12 H, m, CH_2CH_3), 3.05 (6 H, s, CH_3), 3.42–3.58 (8 H, m, CH_2CH_3), 8.25 (2 H, m, phenyl CH), 9.21 (2 H, s, CH=C), 9.45 (2 H, m, phenyl CH), 11.25 (2 H, s, CH=N). CI MS (CH_4): *m/e* 491 (calcd for $C_{32}H_{35}N_5H^+$ 490). FAB MS (3-nitrobenzyl alcohol matrix, 8-keV acceleration): *m/e* 512 (calcd for $C_{32}H_{35}N_5Na^+$ 512). IR (KBr): ν 3420, 2960, 2920, 2860, 1600, 1560, 1540, 1370, 1350, 1255, 1210, 1080, 1050, 980, 940, 905, 750 cm^{-1}. UV/vis ($CHCl_3$) λ_{max} 327.0 (ϵ 30 700) 422.5 (60 500), 692.0 (10 100), 752.0 nm (36 400).

Preparation of Complex 3(Cl). The sp^3 form of the ligand (**1**)[14] (40 mg, 0.08 mmol) was stirred with cadmium chloride (21.4 mg, 0.08 mmol) in chloroform–methanol (150 mL, 2/1 v/v) for 1 day. The dark green reaction mixture was concentrated under reduced pressure on a rotary evaporator and chromatographed through silica gel by using first pure chloroform and then chloroform–methanol (10/1 v/v) as eluents. After several leading red bands were discarded, the dark green band was collected and taken to dryness in vacuo to give **3**(Cl). This material was recrystallized from chloroform–*n*-hexane to give analytically pure **3**(Cl) as a dark green powder in 24% yield. ^{1}H NMR ($CDCl_3$): δ 1.55–1.67 (12 H, m, CH_2CH_3), 3.03 (6 H, s, CH_3), 3.04–3.55 (8 H, m, CH_2CH_3), 8.27 (2 H, m, phenyl CH), 9.23 (2 H, s, CH=C), 9.40 (2 H, m, phenyl CH), 11.30 (2 H, s, CH=N). ^{13}C NMR ($CDCl_3$): δ 9.8, 17.3, 18.1, 19.1, 19.2, 117.6, 117.8, 128.4, 132.7, 138.2, 139.3, 145.4, 146.7, 150.5, 153.5, 155.0. FAB MS (3-nitrobenzyl alcohol matrix, 8-keV acceleration): *m/e* 602 (^{114}Cd, M$^+$, 100), 601 (^{113}Cd, M$^+$, 64), 600 (^{112}Cd, M$^+$, 84). IR (KBr): ν 2950, 2910, 2855, 1635, 1605, 1380, 1255, 1210, 1090, 1010, 795 cm^{-1}. UV/vis: λ_{max} 327.0 (ϵ 32 800), 424.0 (72 700), 704.5 (11 000), 767.5 nm (41 200). Anal. Calcd for $C_{32}H_{34}N_5CdCl\cdot{}^1/_2H_2O$: C, 59.54; H, 5.46; N, 10.85. Found: C, 59.78; H, 5.32; N, 10.80.

Preparation of Complex 3(NO_3). The sp^3 form of the ligand **1**[14] (40 mg, 0.08 mmol) was stirred with cadmium nitrate tetrahydrate (31 mg, 0.1 mmol) in chloroform–methanol (150 mL, 1/2 v/v) for 1 day. The dark green reaction mixture was then concentrated and purified by chromatography on silica gel as described above. The resulting crude material was then recrystallized from chloroform–*n*-hexane to give analytically pure **3**(NO_3) in 27% yield.[46] ^{1}H NMR ($CDCl_3$): δ 1.55–1.70 (12 H, m, CH_2CH_3), 3.04 (6 H, s, CH_3), 3.42–3.55 (8 H, m, CH_2CH_3), 8.27 (2 H, m, phenyl CH), 9.20 (2 H, s, CH=C), 9.30 (2 H, m, phenyl CH), 11.07 (2 H, s, CH=N). FAB MS (3-nitrobenzyl alcohol matrix, 8-keV acceleration): *m/e* 602 (^{114}Cd, M$^+$, 100), 601 (^{113}Cd, M$^+$, 61), 600 (^{112}Cd, M$^+$, 87). IR (KBr): ν 2960, 2920, 1600, 1550, 1440, 1375, 1200, 1130, 1075, 1040, 975, 930, 900, 740 cm^{-1}. UV/vis: λ_{max} 328.0 (ϵ 39 900), 425.0 (82 800), 706.0 (14 400), 770 nm (49 800). Anal. Calcd for $C_{32}H_{34}N_5CdNO_3\cdot{}^1/_2H_2O$: C, 57.19; H, 5.25; N, 12.50. Found: C, 57.12; H, 5.19; N, 11.80.

Preparation and Isolation of Complex 4b(NO_3). The sp^3 form of the ligand **1** (40 mg, 0.08 mmol) was stirred with cadmium nitrate tetrahydrate (31 mg, 0.1 mmol) in chloroform–methanol (150 mL, 1/2 v/v) for 1 day. The dark green reaction mixture was concentrated on a rotary evaporator and chromatographed through Sephadex by using first neat chloroform and then chloroform–methanol (10/1 v/v) as eluents. After several leading red bands were discarded, the dark green band was collected and concentrated to give a dark green solid. This was recrystallized from chloroform–*n*-hexane to give a mixture of crystalline and noncrystalline solids in 27% yield. Data for this bulk material is as follows. ^{1}H NMR ($CDCl_3$): δ 1.55–1.72 (12 H, m, CH_2CH_3), 3.04 (6 H, s, CH_3), 3.45–3.58 (8 H, m, CH_2CH_3), 6.4 (ca. $^3/_5$ H, br s, BzIm), 6.81 (ca. $^6/_5$ H, br s, BzIm), 7.27 (ca. $^6/_5$ H, s, BzIm), 8.29 (2 H, m, phenyl CH), 9.21 (2 H, s, CH=C), 9.32 (2 H, m, phenyl CH), 11.08 (2 H, s, CH=N). FAB MS (3-nitrobenzyl alcohol matrix, 8-keV acceleration): *m/e* 602 (^{114}Cd, M$^+$, 100), ^{113}Cd, M$^+$, 67), 600 (^{112}Cd, M$^+$, 78). IR (KBr): ν 2970, 2935, 2875, 1560, 1382, 1356, 1300, 1258, 1212, 1085, 1050, 985, 945, 910, 755 cm^{-1}. UV/vis: λ_{max} 325.0 (ϵ 29 000), 425.0 (64 400), 710.5 (9800), 767.5 (38 500). Anal. Found: C, 42.42; H, 4.28; N, 10.34. Calcd for $C_{32}H_{34}N_5CdNO_3\cdot{}^1/_2H_2O$: C, 57.19; H, 5.25; N, 12.50. Calcd for $C_{32}H_{34}N_5CdNO_3BzIm\cdot CHCl_3$: C, 53.35; H, 4.59; N, 12.44. Calcd for $C_{32}H_{34}N_5CdNO_3\cdot 3CHCl_3$: C, 41.26; H, 3.66; N, 8.25. The single crystal of **4b** used for the X-ray structure determination was isolated from residual noncrystalline material following a second recrystallization, which involved layering a concentrated solution of the above crude material in $CDCl_3$ with *n*-hexane and letting stand for several months in the refrigerator.

Preparation of Complex 5a(NO_3). In a fashion similar to that used to prepare the crude cadmium-containing complex described above, the sp^3 form of the ligand **1** was treated with cadmium nitrate tetrahydrate and purified on Sephadex. To a ca. 0.7 mL, 0.005 M sample of this product in $CDCl_3$ was added 25 μL of py-d_5. The resulting solution was layered with *n*-hexane, and the mixture was placed in the refrigerator. After several months, green crystals were isolated in nearly quantitative yield. The molecular composition of these crystals was determined, on the basis of the single-crystal X-ray diffraction analysis reported earlier,[11] to be **5a**(NO_3)·$CHCl_3$. ^{1}H NMR ($CDCl_3$–py-d_5): δ 1.55–1.70 (12 H, m, CH_2CH_3), 3.22 (3 H, s, CH_3), 3.45–3.56 (8 H, m, CH_2CH_3), 8.40 (2 H, m, phenyl CH), 9.32 (2 H, s, CH=C), 9.75 (2 H, m, phenyl CH), 11.62 (2 H, s, CH=N). UV/vis ($CHCl_3$–pyr, 10/1 v/v): λ_{max} 321.5 (ϵ 45 000), 426.5 (79 000), 700.5 (13 500), 765.5 nm (51 900).

^{1}H NMR Titration of 3(NO_3) with BzIm or py-d_5. Rigorously purified complex **3**(NO_3) was dried at 80 °C under reduced pressure (1 mmHg) for 1 day. Starting samples for titration were then prepared by dissolving this five-coordinate complex (3.32 mg, 0.005 mmol) in 0.7–0.75 mL of $CDCl_3$ and transferring quantitatively to an NMR tube. To such samples were then added increasing aliquots of either BzIm or py-d_5 (as solutions of known concentration in $CDCl_3$), and the chemical shifts of the "meso"-like imine (CH=N) protons were recorded at 27 °C. Control experiments were also carried out by adding known quantities of CF_3CO_2H, D_2O, and NH_4NO_3 to similar stock solutions of **3**(NO_3). In these various ^{1}H NMR titrations the absolute chemical shifts for any given base to ligand ratio were found to vary by less than 0.05 ppm between independent runs, with the values of $\delta - \delta_0$, the critical observable used for the K_{eq} determinations (see below), being found to vary even less (generally $\leq$0.003 ppm).

Determination of Binding Constants. Inspection of Figures 5 and 6 shows that the binding of BzIm to cation **3** may be considered as two well-separated equilibrium processes. The chemical shift data obtained for the imine signals as a function of added BzIm were thus analyzed as such at both very low and very high conversion: Standard Scatchard (single reciprocal) plots[38] were constructed by plotting $(\delta - \delta_0)/[\mathrm{BzIm}]$ vs $\delta - \delta_0$ according to eq 4 (which corresponds to eq 5.13 of ref 38), K

$$(\delta - \delta_0)/[\mathrm{BzIm}] = -K(\delta - \delta_0) + (\delta_\infty - \delta_0)K \qquad (4)$$

being obtained as the absolute value of the slope and the term $(\delta_\infty - \delta_0)K$ as the intercept. Here δ is the observed chemical shift, δ_0 is the initial chemical shift of the pure five- or six-coordinate starting complex (**3**(NO_3) or **4b**(NO_3)), δ_∞ is the chemical shift calculated for the final mono- and bisligated complexes **4b**(NO_3) and **5b**(NO_3), K is the equilibrium constant in question, and [BzIm] is the concentration of free, uncomplexed benzimidazole. In both the low- and high-conversion regimes, it proved necessary to correct for bound benzimidazole so as to obtain valid expressions for [BzIm] in terms of added benzimidazole ($[\mathrm{BzIm}]_0$). This was done in a straightforward manner according to the expressions given in eq 5 and 6, where $[\mathrm{lig}]_0$ represents the concentration

$$[\mathrm{BzIm}] = [\mathrm{BzIm}]_0 - [\mathrm{lig}]_0(\delta - \delta_0)/(\delta_\infty - \delta_0) \quad \text{low } [\mathrm{BzIm}]_0 \qquad (5)$$

$$[\mathrm{BzIm}] \cong [\mathrm{BzIm}]_0 - [\mathrm{lig}]_0 \quad \text{high } [\mathrm{BzIm}]_0 \qquad (6)$$

of the starting five-coordinate ligand **3**(NO_3). With use of these corrected values for [BzIm], straight-line Scatchard plots were obtained with $R \geq 0.99$ and 0.98, respectively, for the low- and high-$[\mathrm{BzIm}]_0$ regimes, giving values of K_1 and K_2 of 1.80×10^4 and 12.9 M^{-1}, respectively (see supplementary material). We consider the value for K_1 to be quite reliable (estimated error $\leq$15%); the low solubility of BzIm and the

(46) This material has been further characterized by preliminary ^{113}Cd NMR studies in the solid state (Kennedy, M. A.; Ellis, P. D.; Murai, T.; Sessler, J. L. Unpublished results). The isotropic chemical shift of this complex (**3**(NO_3)), σ = 191 ppm relative to solid cadmium perchlorate, is shielded by $\simeq$200–300 ppm relative to "normal" cadmium porphyrins such as CdTPP[25] (σ = 399 ppm[47]) or CdPPIXDME[25] (σ = 480 ppm[48]). This difference may reflect the increased shielding caused by the presence of an additional pair of electrons within the binding core of the "expanded" porphyrin-like macrocyclic ligand. A simulation of magic-angle-spinning spectra, from the theory of Maricq and Waugh,[49] yields an anisotropy of $\Delta\sigma$ = 207.6 and asymmetry of η = 0.01, indicative of a system with a $\geq$3-fold axis of symmetry. In addition, the eigenvalues of the chemical shift tensor were found to be σ_{11} = 120.6 ppm, σ_{22} = 123 ppm, and σ_{33} = 329.6 ppm.

(47) Jakobsen, H. J. *J. Am. Chem. Soc.* **1982**, *104*, 7442–7542.

(48) Kennedy, M. A.; Ellis, P. D. Submitted for publication in *J. Biol. Chem.*

(49) Maricq, M.; Waugh, J. S. *J. Chem. Phys.* **1979**, *70*, 3300–3316.

Table I. Crystallographic Data for **4b**$(NO_3)\cdot CHCl_3$

chem formula	$C_{40}H_{41}N_8O_3Cl_3Cd$	fw	900.57
		space group	$P\bar{1}$ (No. 2)
a, Å	11.276 (4)	T, °C	−110
b, Å	12.845 (3)	λ(Mo Kα), Å	0.71073
c, Å	14.913 (4)	ρ_{obs}, g/cm^3	1.48
α, deg	84.82 (2)	(−110 °C)	
β, deg	69.57 (2)	μ, cm^{-1}	7.867
γ, deg	85.84 (2)	transmission coeff	0.8533–0.9557
V, Å^3	2014 (1)	$R(F)$	0.0781
Z	2	$R_w(F)$	0.114

resulting incomplete nature of the titration associated with the formation of **5b**(NO_3), however, makes the value obtained for K_2 somewhat more approximate (estimated error ≤25%).[50]

The changes in the imine proton chemical shift as a function of added [py], shown in Figures 7 and 8, indicate a clear absence of two distinct binding regimes. Moreover, as expected, attempts to fit the data as a simple monoligation process (to give 6 CN material) according to eq 1 did not work. It therefore proved necessary to analyze the data in terms of two concurrent equilibrium processes. This was done by using the convenient iterative procedure outlined by Connors.[38] Here the equations of interest, corresponding to eq 4.31 and 4.32 of ref 38, as adopted for NMR analyses, are

$$1/[py] - K_1\Delta_{11}/(\delta - \delta_0) = K_1K_2[py]\{\Delta_{12}/(\delta - \delta_0) - 1\} - K_1 \quad (7)$$

$$(\delta - \delta_0)\{1 + K_1[py] + K_1K_2[py]^2\}/[py] = K_1K_2\Delta_{12}[py] + K_1\Delta_{11} \quad (8)$$

where δ is the observed chemical shift, δ_0 is the initial chemical shift of the pure five-coordinate starting complex **3**(NO_3), Δ_{11} is the total chemical shift difference corresponding to the formation of the pure putative monoligated six-coordinate species, Δ_{12} is the total chemical shift corresponding to the formation of the bisligated cationic species **5a** from the initial five-coordinate material, and [py] is the free pyridine concentration. A precise expression for [py] is given by eq 9,[38] where $[py]_0$ is the

$$[py]_0 = [py] + [lig]_0(K_1[py] + 2K_1K_2[py]^2)/(1 + K_1[py] + K_1K_2[py]^2) \quad (9)$$

concentration of total added pyridine and $[lig]_0$ represents the concentration of the starting five-coordinate ligand **3**(NO_3). Inspection of the binding isotherm (Figure 8), however, suggested that the approximation $[py] \cong [py]_0$ would be reasonably valid over much of the titration range. Initial iterative solutions of eq 7 (plot of $1/[py] - K_1\Delta_{11}/(\delta - \delta_0)$ vs $[py]\{\Delta_{12}/(\delta - \delta_0) - 1\}$, giving K_1K_2 and $-K_1$ as the slope and intercept, respectively) and eq 8 (plot of $(\delta - \delta_0)\{1 + K_1[py] + K_1K_2[py]^2\}/[py]$ vs [py], giving $K_1K_2\Delta_{12}$ and $K_1\Delta_{11}$ as the slope and intercept, respectively) were therefore made by using this greatly simplifying assumption. They converged quickly to give initial, uncorrected values of $K_1 \cong 1.5$ M^{-1} and $K_1K_2 = 308$ M^{-2}. These values confirmed that, under the conditions of the experiment (where [**3**(NO_3)] ≅ 0.005 M), the approximation $[py] \cong [py]_0$ is valid to within ≤4% in the regime of greatest interest, namely $3 <$ [pyridine]/[ligand] < 10 and 0.005 M in **3**(NO_3). When corrections are made for this small percentage, final values of $K_1 \cong 1.6$ M^{-1} and $K_1K_2 = 315$ M^{-2} are obtained (see supplementary material). We consider it important to stress that although the value of K_1K_2 is well determined (estimated error ≤10%), the nature of the data does not allow K_1 (and hence K_2) to be defined with precision (estimated error ≅50%). This uncertainty, however, does not detract from the central conclusions of this paper.

X-ray Experimental Data Collection for Complex 4b. For **4b**$(NO_3)\cdot CHCl_3$ ($C_{40}H_{41}N_8O_3Cl_3Cd$) $M_r = 900.57$. The data crystal was a very dark green plate of dimensions 0.06 × 0.22 × 0.44 mm, which was grown by slow diffusion from $CHCl_3$–hexane and separated from the accompanying noncrystalline material as described above. The data were collected on a Nicolet R3 diffractometer, with a graphite monochromator, using Mo Kα radiation (λ = 0.71069 Å) and a Nicolet LT-2 low-temperature delivery system (163 K). Lattice parameters were obtained from least-squares refinement of 26 reflections with $19.2° < 2\theta < 24.4°$. Data were collected by using the ω-scan technique (7191 reflections, 6566 unique, $R_{int} = 0.064$), 2θ range 4.0–50.0°, 1.2° ω scan at 3–6°/min (h = 0–14, k = −15 to 15, l = −18 to 18). Four reflections (−2,2,0; 323; 2,−3,−1; −1,0,−4) were remeasured every 146 reflections to monitor instrument and crystal stability. Decay correction range on I was 0.9863–1.076. Data were also corrected for Lp effects and absorption (based on crystal shape; transmission factor range 0.8533–0.9557, μ = 7.867 cm^{-1}). Reflections having $F_o < 6\sigma(F_o)$ were considered unobserved (3272 reflections). The structure was solved by heavy-atom and Fourier methods and refined by full-matrix least-squares procedures in blocks of 253 and 287 with anisotropic thermal parameters for the non-H atoms (except O3a of the disordered NO_3^- group and the terminal C atoms of the disordered ethyl groups of one pyrrole ring, C29 [site occupancy factor 0.44 (2)], C29A, C31 [site occupancy factor 0.37(2)] and C31a. Nitrate

(50) These data could be analyzed by using the iterative approach used for pyridine complexation. Values of K_1 and K_1K_2 of 2.0×10^4 M^{-1} and 1.9×10^5 M^{-2} were obtained by using this approach.

Table II. Fractional Coordinates and Isotropic or Equivalent Isotropic[a] Thermal Parameters (Å^2) for Non-Hydrogen Atoms of **4b**$(NO_3)\cdot CHCl_3$

atom	x	y	z	U
Cd	0.37392 (8)	0.12411 (6)	0.04542 (7)	0.0573 (4)
N1	0.5259 (9)	0.1813 (7)	0.1140 (9)	0.065 (5)
C2	0.5321 (13)	0.1503 (10)	0.2032 (11)	0.062 (6)
C3	0.6213 (12)	0.2115 (11)	0.2219 (10)	0.064 (6)
C4	0.6661 (11)	0.2783 (9)	0.1439 (11)	0.061 (6)
C5	0.6066 (12)	0.2575 (9)	0.0765 (11)	0.060 (6)
C6	0.6340 (12)	0.3124 (9)	−0.0106 (12)	0.065 (7)
C7	0.5828 (11)	0.3039 (8)	−0.0848 (11)	0.063 (6)
N8	0.4929 (9)	0.2314 (7)	−0.0754 (8)	0.056 (4)
C9	0.4750 (12)	0.2437 (10)	−0.1581 (11)	0.070 (6)
C10	0.5492 (14)	0.3233 (11)	−0.2225 (10)	0.075 (6)
C11	0.6178 (12)	0.3604 (9)	−0.1782 (11)	0.069 (6)
C12	0.3827 (14)	0.1784 (12)	−0.1763 (10)	0.073 (6)
N13	0.3236 (10)	0.1169 (8)	−0.1068 (8)	0.057 (4)
C14	0.2359 (11)	0.0438 (11)	−0.1074 (10)	0.063 (6)
C15	0.1851 (13)	0.0468 (12)	−0.1834 (10)	0.072 (6)
C16	0.1028 (14)	−0.0250 (12)	−0.1825 (10)	0.067 (6)
C17	0.0648 (13)	−0.0982 (12)	−0.1067 (11)	0.071 (7)
C18	0.1077 (12)	−0.1040 (9)	−0.0331 (11)	0.074 (7)
C19	0.1952 (12)	−0.0304 (8)	−0.0304 (11)	0.064 (6)
N20	0.2428 (10)	−0.0258 (9)	0.0420 (9)	0.065 (5)
C21	0.2112 (13)	−0.0873 (9)	0.1201 (11)	0.065 (6)
C22	0.2643 (12)	−0.0711 (9)	0.1918 (11)	0.065 (7)
N23	0.3510 (10)	0.0013 (6)	0.1716 (9)	0.061 (5)
C24	0.3782 (14)	0.0029 (10)	0.2535 (13)	0.076 (7)
C25	0.3076 (14)	−0.0727 (10)	0.3260 (12)	0.080 (7)
C26	0.2349 (15)	−0.1183 (9)	0.2854 (11)	0.073 (7)
C27	0.4669 (13)	0.0715 (10)	0.2649 (11)	0.067 (6)
C28	0.6508 (14)	0.2018 (13)	0.3139 (11)	0.084 (7)
C29	0.553 (5)	0.234 (4)	0.400 (3)	0.105 (15)
C29a	0.590 (3)	0.282 (2)	0.381 (2)	0.082 (8)
C30	0.765 (2)	0.3611 (12)	0.1304 (13)	0.088 (8)
C31a	0.710 (3)	0.450 (2)	0.194 (2)	0.101 (9)
C31	0.704 (3)	0.475 (2)	0.134 (2)	0.040 (7)
C32	0.7108 (13)	0.4478 (10)	−0.2122 (11)	0.072 (6)
C33	0.6487 (14)	0.5579 (11)	−0.1933 (13)	0.088 (8)
C34	0.553 (2)	0.3512 (14)	−0.3236 (10)	0.096 (8)
C35	0.132 (2)	−0.1983 (11)	0.3305 (13)	0.093 (8)
C36	0.305 (2)	−0.0887 (12)	0.4286 (11)	0.084 (8)
C37	0.229 (2)	−0.007 (2)	0.4904 (14)	0.125 (11)
N1a	0.2036 (10)	0.2375 (6)	0.1132 (8)	0.059 (5)
C2a	0.1817 (13)	0.3278 (11)	0.060 (2)	0.095 (9)
N3a	0.0853 (13)	0.3834 (8)	0.1207 (14)	0.101 (8)
C4a	0.0536 (12)	0.3373 (11)	0.2074 (14)	0.073 (7)
C5a	−0.043 (2)	0.3615 (13)	0.300 (2)	0.103 (11)
C6a	−0.056 (2)	0.296 (2)	0.378 (2)	0.116 (12)
C7a	0.0178 (15)	0.1969 (15)	0.3762 (10)	0.089 (7)
C8a	0.1056 (14)	0.1750 (12)	0.2886 (11)	0.070 (7)
C9a	0.1212 (11)	0.2418 (9)	0.2079 (10)	0.053 (5)
Cl1	0.3144 (6)	0.4520 (4)	0.5507 (4)	0.129 (3)
Cl2	0.3058 (12)	0.2261 (8)	0.5862 (6)	0.118 (5)
Cl3	0.1613 (13)	0.3391 (13)	0.4877 (8)	0.165 (8)
Cl2a	0.056 (2)	0.4327 (14)	0.5339 (13)	0.155 (10)
Cl3a	0.2064 (15)	0.2450 (12)	0.5529 (14)	0.157 (9)
C1c	0.198 (3)	0.357 (2)	0.5834 (15)	0.152 (15)
N1b	0.9690 (14)	0.6403 (9)	0.1553 (10)	0.073 (6)
O1	0.985 (3)	0.588 (2)	0.079 (2)	0.072 (11)
O2	0.943 (4)	0.734 (2)	0.167 (2)	0.17 (2)
O3	0.958 (3)	0.587 (2)	0.233 (2)	0.123 (14)
O1a	0.853 (3)	0.660 (4)	0.199 (3)	0.19 (2)
O2a	1.043 (3)	0.598 (3)	0.089 (3)	0.065 (13)
O3a	1.030 (5)	0.676 (4)	0.173 (3)	0.16 (2)

[a] For anisotropic atoms, the U value is U_{eq}, calculated as $U_{eq} = {}^1/_3\sum_i\sum_j U_{ij}a_i^*a_j^*A_{ij}$, where A_{ij} is the dot product of the ith and jth direct-space unit cell vectors.

Table III. Bond Lengths (Å) and Angles (deg) for Non-Hydrogen Atoms of Cation **4b**

atom 1	atom 2	atom 3	1–2	1–2–3	atom 1	atom 2	atom 3	1–2	1–2–3
C2	N1	C5	1.38 (2)	107.2 (13)	N20	C19	C18		125.7 (12)
C5	N1		1.33 (2)		C14	C19	C18		118 (2)
C3	C2	C27	1.43 (2)	124 (2)	C21	N20	C19	1.30 (2)	124.2 (13)
C3	C2	N1		109.5 (11)	C22	C21	N20	1.43 (3)	118.3 (13)
C27	C2	N1	1.37 (2)	126.3 (15)	N23	C22	C26	1.34 (2)	113 (2)
C4	C3	C28	1.35 (2)	129.3 (14)	N23	C22	C21		118.0 (13)
C4	C3	C2		105.9 (14)	C26	C22	C21	1.41 (2)	129.1 (12)
C28	C3	C2	1.51 (2)	124.7 (12)	C24	N23	C22	1.36 (2)	104.7 (12)
C5	C4	C30	1.44 (3)	126.9 (13)	C25	C24	C27	1.44 (2)	125 (2)
C5	C4	C3		107.8 (12)	C25	C24	N23		111.1 (14)
C30	C4	C3	1.55 (2)	125 (2)	C27	C24	N23	1.44 (2)	123.9 (12)
C6	C5	N1	1.37 (2)	129 (2)	C26	C25	C36	1.37 (3)	127.9 (13)
C6	C5	C4		121.7 (12)	C26	C25	C24		105 (2)
N1	C5	C4		109.5 (13)	C36	C25	C24	1.52 (3)	127 (2)
C7	C6	C5	1.43 (3)	129.2 (12)	C35	C26	C22	1.54 (2)	124 (2)
N8	C7	C11	1.39 (2)	110.7 (14)	C35	C26	C25		129 (2)
N8	C7	C6		121.3 (12)	C22	C26	C25		106.3 (12)
C11	C7	C6	1.45 (2)	127.8 (12)	C2	C27	C24		130 (2)
C9	N8	C7	1.31 (2)	103.3 (11)	C29	C28	C3	1.44 (4)	118 (3)
C10	C9	C12	1.43 (2)	127 (2)	C29a	C28	C3	1.46 (3)	115 (2)
C10	C9	N8		113.6 (14)	C31a	C30	C4	1.51 (3)	112 (2)
C12	C9	N8	1.49 (2)	119.7 (11)	C31	C30	C4	1.57 (3)	111 (2)
C11	C10	C34	1.32 (2)	127.8 (13)	C33	C32	C11	1.54 (2)	114.0 (11)
C11	C10	C9		106.7 (14)	C37	C36	C25	1.47 (2)	114 (2)
C34	C10	C9	1.51 (2)	125 (2)	C9a	N1A	C2A	1.40 (2)	108.5 (10)
C32	C11	C7	1.52 (2)	125 (2)	C2a	N1A		1.40 (2)	
C32	C11	C10		129.1 (15)	N3a	C2A	N1A	1.35 (2e	107 (2)
C7	C11	C10		105.7 (11)	C4a	N3A	C2A	1.31 (3)	109.4 (14)
N13	C12	C9	1.26 (2)	115.2 (15)	C5a	C4A	C9A	1.47 (3)	115 (2)
C14	N13	C12	1.41 (2)	126.1 (14)	C5a	C4A	N3A		133.3 (14)
C15	C14	C19	1.43 (2)	119.5 (13)	C9a	C4A	N3A	1.40 (2)	111.2 (13)
C15	C14	N13		121.7 (12)	C6a	C5A	C4A	1.34 (3)	120 (2)
C19	C14	N13	1.39 (2)	118.7 (14)	C7a	C6A	C5A	1.47 (3)	124 (2)
C16	C15	C14	1.35 (2)	120.2 (13)	C8a	C7A	C6A	1.37 (2)	115 (2)
C17	C16	C15	1.37 (2)	119 (2)	C9a	C8A	C7A	1.38 (2)	121.7 (14)
C18	C17	C16	1.34 (3)	123 (2)	N1a	C9A	C4A		103.7 (12)
C19	C18	C17	1.43 (2)	120.0 (13)	N1a	C9A	C8A		132.1 (11)
N20	C19	C14	1.37 (2)	116.6 (12)	C4a	C9A	C8A		124.1 (13)

was disordered about two orientations of the N atom (N1b) with a site occupancy factor for the minor orientation (O atoms labeled with a) of 0.45 (2). H atoms were calculated and refined with isotropic thermal parameters riding on the relevant C atom. $CHCl_3$ solvent is disordered by rotation about a C–Cl bonding axis (C1C–Cl1) with a site occupancy factor for the minor component (Cl atoms labeled with a) of 0.43 (2). Due to the disorder, the chloroform H atom position was not calculated. $\sum w(|F_o| - |F_c|)^2$ was minimized, where $w = 1/[(\sigma(F_o))^2 + 0.0118(F^2)]$ and $\sigma(F_o) = 0.5kI^{-1/2}(\sigma(I))$. Intensity, I, is given by $(I_{peak} - I_{background})$(scan rate), and k is the correction due to Lp effects, absorption, and decay. $\sigma(I)$ is estimated from counting statistics; $\sigma(I) = (I_{peak} + I_{background})^{1/2}$(scan rate). Final $R = 0.0781$ for 3294 reflections, $R_w = 0.114$ ($R_{all} = 0.143$, $R_{w,all} = 0.176$) and goodness of fit = 1.00. Maximum $|\Delta/\sigma| < 0.1$ in the final refinement cycle, and the minimum and maximum peaks in the final ΔF map were −0.97 and 1.69 e/Å^3, respectively (in the region of the Cd atom). Data reduction, structure solution, and initial refinement were accomplished by using Nicolet's SHELXTL-PLUS[51] software package. The final refinement was done by using SHELX76.[52] Neutral atom scattering factors for the non-H atoms were from Cromer and Mann,[53] with anomalous-dispersion corrections from Cromer and Liberman,[54] while scattering factors for the H atoms were from Stewart, Davidson, and Simpson;[55] linear absorption coefficients were taken from ref 56. The least-squares planes program was supplied by Cordes;[57] other computer programs were from reference 11 of Gadol and Davis.[58]

Acknowledgment. We are grateful to the Texas Advanced Research Program, the Camille and Henry Dreyfus Foundation (New Faculty Award to J.L.S., 1984), the National Science Foundation (Presidential Young Investigator Award J.L.S., 1986), and the Procter and Gamble Co. for financial support. We thank Mike Kennedy of the University of South Carolina for helpful discussions, Miguel Rosingana and Mike Cyr of the University of Texas for synthetic assistance, and Greg Hemmi and Dr. Ben Shoulders for help with the NOE experiments.

Supplementary Material Available: Additional views of cation **4b**, tables of anisotropic thermal parameters for the non-H atoms of **4b**-(NO_3)·$CHCl_3$ (Table 1), fractional coordinates and isotropic thermal parameters for the H atoms (Table 2), bond lengths and angles for the disordered $CHCl_3$ and NO_3^- groups (Table 3), bond lengths and angles for H atoms (Table 4), and least-squares planes (Table 5), the UV–visible spectrum of $3(NO_3)$, and additional ^{1}H NMR spectra and listings of representative chemical shift data for the titration of $3(NO_3)$ with BzIm and pyridine and appropriate plots for the associated K_{eq} calculations (29 pages); a table of observed and calculated structure factor amplitudes (Table 6) (40 pages). Ordering information is given on any current masthead page.

(51) "SHELXTL-PLUS"; Nicolet: Madison, WI, 1987.
(52) Sheldrick, G. M. "SHELX76: A Program for Crystal Structure Determination"; University of Cambridge: Cambridge, England, 1976.
(53) Cromer, D. T.; Mann, J. B. *Acta Crystallogr.* **1968**, *A24*, 321–324.
(54) Cromer, D. T.; Liberman, D. *J. Chem. Phys.* **1970**, 53, 1891–1898.
(55) Stewart, R. F.; Davidson, E. R.; Simpson, W. T. *J. Phys. Chem.* **1965**, *42*, 3175–3187.
(56) *International Tables for X-ray Crystallography*; Kynoch Press: Birmingham, England, 1974; Vol. IV, p 55.
(57) Cordes, A. W. Personal communication, 1983.
(58) Gadol, S. M.; Davis, R. E. *Organometallics* **1982**, *1* 1607–1613.